Biology of Reproduction, 2018, 99(6), 1171–1183
doi:10.1093/biolre/ioy156
Research Article
Advance Access Publication Date: 11 July 2018

OXFORD

Research Article

WBP2 shares a common location in mouse spermatozoa with WBP2NL/PAWP and like its descendent is a candidate mouse oocyte-activating factor

Lauren E. Hamilton[1], Joao Suzuki[2], Genevieve Acteau[1], Mengqi Shi[1], Wei Xu[1], Marie-Charlotte Meinsohn[2], Peter Sutovsky[3,4] and Richard Oko[1,*]

[1]Department of Biomedical and Molecular Sciences, Queen's University, Kingston, Ontario, Canada; [2]Centre de recherche en reproduction fertilité, Faculté de médecine vétérinaire, Université de Montréal, St. Hyacinthe, Quebec, Canada ; [3]Division of Animal Sciences, College of Food, Agriculture and Natural Resources, University of Missouri, Columbia, Missouri, USA and [4]Department of Obstetrics, Gynecology and Women's Health, School of Medicine, University of Missouri, Columbia, Missouri, USA

*__Correspondence:__ Department of Biomedical and Molecular Sciences, Queen's University, Kingston, K7L 3N6, ON, Canada. Tel: +613-533-2858; Fax: +613-533-2022; E-mail: ro3@queensu.ca

Received 1 June 2017; Revised 6 October 2017; Accepted 12 July 2018

Abstract

The sperm-borne oocyte-activating factor (SOAF) resides in the sperm perinuclear theca (PT). A consensus has been reached that SOAF most likely resides in the postacrosomal sheath (PAS), which is the first region of the PT to solubilize upon sperm–oocyte fusion. There are two SOAF candidates under consideration: PLCZ1 and WBP2NL. A mouse gene germline ablation of the latter showed that mice remain fertile with no observable phenotype despite the fact that a competitive inhibitor of WBP2NL, derived from its PPXY motif, blocks oocyte activation when coinjected with WBP2NL or spermatozoa. This suggested that the ortholog of WBP2NL, WBP2, containing the same domain and motifs associated with WBP2NL function, might compensate for its deficiency in oocyte activation. Our objectives were to examine whether WBP2 meets the developmental criteria established for SOAF and whether it has oocyte-activating potential. Immunoblotting detected WBP2 in mice testis and sperm and immunofluorescence localized WBP2 to the PAS and perforatorium of the PT. Immunohistochemistry of the testes revealed that WBP2 reactivity was highest in round spermatids and immunofluorescence detected WBP2 in the cytoplasmic lobe of elongating spermatids and colocalized it with the microtubular manchette during PT assembly. Microinjection of the recombinant forms of WBP2 and WBP2NL into metaphase II mouse oocytes resulted in comparable rates of oocyte activation. This study shows that WBP2 shares a similar testicular developmental pattern and location with WBP2NL and a shared ability to activate the oocyte, supporting its consideration as a mouse SOAF component that can compensate for a WBP2NL.

Summary Sentence

WBP2 and WBP2NL share sperm location, development origins, and oocyte-activating ability in mouse.

Key words: WBP2, WBP2NL/PAWP, sperm, perinuclear theca, postacrosomal sheath, perforatorium, spermatogenesis, spermiogenesis, microtubular manchette, fertilization, oocyte activation, ICSI, mouse.

Introduction

The most accepted hypothesis for the mechanism of oocyte activation is that following sperm–oocyte plasma membrane fusion the spermatozoon releases a sperm-borne oocyte-activating factor(s) (SOAF) into the oocyte cytoplasm. This model of sperm induced oocyte activation was first introduced in 1990 in two independent investigations [1, 2]. SOAF induces a relatively short lived, large intracellular Ca^{2+} increase as in amphibians or a series of episodic Ca^{2+} oscillations as in mammals [3]. The Ca^{2+} release then initiates a series of signaling events leading to zygotic development and cleavage. Interestingly, although sperm PLCZ1 has recently been shown to be required for the induction of Ca^{2+} oscillations in mouse oocytes, the male *Plcz1* null mice retained some fertility [4], suggesting that Ca^{2+} oscillations might not be obligatory and that an alternative pathway may be involved in oocyte activation.

The discovery of where SOAF resides in eutherian spermatozoa, using mouse as a model, was accomplished by a group of investigators led by Ryuzo Yanagimachi [5–9]. The conclusion was that SOAF can be found in the perinuclear theca (PT) because isolated sperm heads that were divested of all membranous components by extraction with nonionic detergents retained only the PT and nucleus. Nevertheless, on microinjection they were still capable of activating oocytes and participating in normal embryo development. In mouse it appears that SOAF within the PT comprises discrete, heat-sensitive, and heat-stable molecules that are each necessary but not sufficient to activate oocytes [8, 9]. These observations suggest a synergistic action between two or more sperm molecules leading to oocyte activation.

The PT of mammalian spermatozoa is compositionally subdivided into two major regions, the subacrosomal layer (SAL-PT), including the outer periacrosomal layer lying over the equatorial segment, and the postacrosomal sheath (PAS-PT) [10–13]. It was initially observed that local PAS solubilization of the PT was sufficient to elicit full oocyte activation during IVF [14]. Utilizing N-butyldeoxynojirimycin (NB-DNJ) treated mice that fail to form a sperm acrosome, equatorial segment, and SAL-PT [15], it was found that the PAS-PT was still assembled in the affected elongated spermatids [16] coincident with the retained ability of the affected spermatozoa to fully activate the oocyte during ICSI [17]. These results imply that that the PAS region of the PT most likely houses SOAF.

Mouse spermatids begin to acquire oocyte-activating ability only in the elongation phase of spermiogenesis [5] indicating that SOAF is expressed and assembled during this phase. This is not surprising considering that the transport process and assembly of proteins making up the murid and bovine PAS-PT is initiated at the beginning and completed at the end of the spermatid elongation [16, 18]. Thus, the developmental timeline of oocyte-activating ability in spermatids corresponds with the assembly of the PAS-PT.

One of the two candidate SOAF proteins in mammals is PAS WW-domain binding protein (PAWP/WBP2NL), an evolutionarily conserved, sperm-specific protein component of the PAS-PT [19]. WBP2NL is expressed and assembled in elongating spermatids and resides in the PAS-PT [16], consistent with the postulated development and location of SOAF. WBP2NL shares sequence homology with the N-terminal half of WW-domain binding protein 2 (WBP2), while the C-terminal half contains functional PPXY motifs also found in WBP2 [19]. The PPXY motifs, identified in molecules mediating protein–protein interactions, bind to WWI domains found in a variety of cellular signaling proteins [20, 21]. WW domains are small functional domains, named after two highly conserved tryptophan residues, which mediate protein–protein interactions in a similar fashion to Src homology 3 domains [21]. The PPXY-WW1 domain interaction is believed to play an essential role in WBP2NL's oocyte-activating ability because whole sperm-, recombinant WBP2NL-, WBP2NL cRNA-, or PT extract-induced oocyte activation is blocked by coinjection of a synthetic peptide derived from the PPXY motif of WBP2NL [19, 22, 23].

From the competitive inhibition results obtained with the PPXY peptide during murine, human, bovine, and porcine ICSI it appeared as though no other potential SOAF in sperm could compensate for sperm WBP2NL-induced oocyte activation. The conclusion was therefore reached that WBP2NL was required for oocyte activation. Surprisingly *Wbp2nl* knockout mice remain fertile [24] indicating that there may be another PPXY containing SOAF protein that is able to compensate for a lack of WBP2NL in the knockout mice. Since *Wbp2nl* evolved from the *Wbp2* gene (see http://www.ensembl.org/Multi/GeneTree/Image?gt=ENSGT00530000063718), which is abundantly transcribed in the testis, it may be able to substitute for a sperm-WBP2NL deficiency in oocyte activation. This study aims to show that WBP2 follows a similar developmental pattern as WBP2NL in mouse spermiogenesis, occupies a similar location as WBP2NL in mouse spermatozoa, and is capable of inducing oocyte activation, thus qualifying it for consideration as a candidate SOAF protein in mouse.

Materials and methods

Animals

Mature male mice were purchased from Charles River Laboratories (Charles River, St-Constant, QC, Canada). All procedures using mice in this study were conducted under Animal Utilization Protocols approved by the Queen's Animal Care Committee, and complied with the Guidelines of Canada Council on Animal Care. The testes and epididymides from bulls were obtained from Hilts Butcher Shop Ltd in Norwood, ON. Human sperm and testes samples were generously donated from Dr Claude Gagnon, Department of Urology, Reproductive Medicine, Department of Urology, McGill University Health Centre. Fertile, nontransgenic boar sperm samples were collected at the National Swine Resource and Research Center and processed at the Division of Animal Sciences, College of Food, Agriculture and Natural Resources, both at the University of Missouri, Columbia, MO.

Sperm extraction from bull epididymides

Epididymides were submerged in 25 mM Tris-buffered saline (TBS) (pH 7.5–8) containing phenyl methylsulfonyl fluoride (PMSF) and cut by a razor several times to allow spermatozoa to diffuse into the suspension. Spermatozoa were separated from epididymal tissue by filtration through 80 μm Nytex netting, followed by centrifugation at 1000 g for 10 min at room temperature, and resuspension in TBS for washing. The sperm pellets were then used directly or frozen at –80°C until needed.

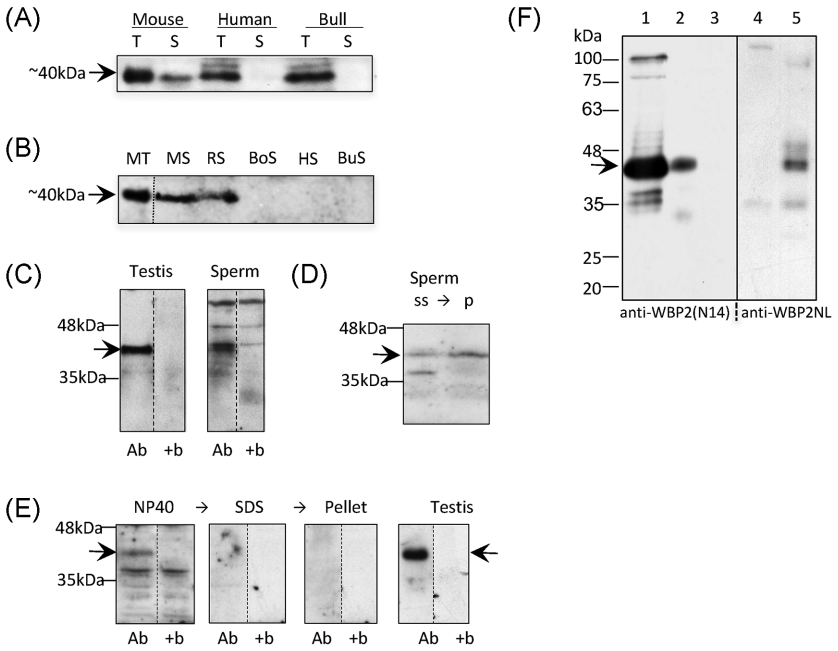

Figure 1. Presence of WBP2 in mouse testis and sperm. (A) WBP2 labeling of a 10% SDS polyacrylamide gel transferred to PVDF. Anti-WBP2 (N-14) antibody labels a band around 40kDa (arrow) in the testis (T) of mouse, human and bull. This band is also present in the mouse sperm (S), but not human or bull spermatozoa. (B) Comparison of the presence of WBP2 in the spermatozoa of different mammalian species. Anti-WBP2 (ProteinTech) antibody labels a band of ~40 kDa (arrow) in mouse testis (MT), and mouse (MS) and rat spermatozoa (RS); however, the band is not present in boar (BoS), human (HS) or bull (BuS) spermatozoa. Each lane, except the MT, was loaded with 7.5 million spermatozoa. All dashed lines in this and subsequent figures represent cuts from adjacent lanes of the same western membranes. The adjacent lanes in subsequent figures were loaded with the same sample but after transfer, they were incubated under different conditions, usually with the addition of a blocking peptide. (C) The immunoreactivity of the 40kDa band (arrow) in both mouse testis and spermatozoa is absent when the anti-WBP2 antibody (Ab) is preincubated with the WBP2 (N-14) blocking peptide (+b). (D) Comparison of relative content of WBP2 (arrow) in sonicated mouse sperm supernatant (ss) and resulting sperm pellet (p) after separation by centrifugation. (E) western blot showing that WBP2 (arrow) is completely extractable from mouse spermatozoa when incubated in nonionic detergent (NP-40). Subsequent extraction in SDS of the NP-40 extracted sperm pellet was devoid of WBP2 as well as its sperm pellet. Testis was used as a positive control and marker. Ab, Anti-WBP2 (N-14) antibody; +b, antibody plus specific blocking peptide. (F) Comparison of anti-WBP2 (N14) and anti-WBP2NL antibody labeling on westerns of mouse sperm NP-40 extracts and NP-40 extracted sperm pellets. Lane 1; Control mouse testis labeled with anti-WBP2 antibody. Lanes 2 and 4: Mouse sperm NP-40 extracts incubated with anti-WBP2 and anti-WBP2NL antibodies, respectively. Lanes 3 and 5: NP-40 extracted sperm pellets incubated with anti-WBP2 and anti-WBP2NL antibodies, respectively. Note there is no immunocrossreactivity detected between these antibodies. Migration levels of molecular mass standards are denoted on the side in kDa.

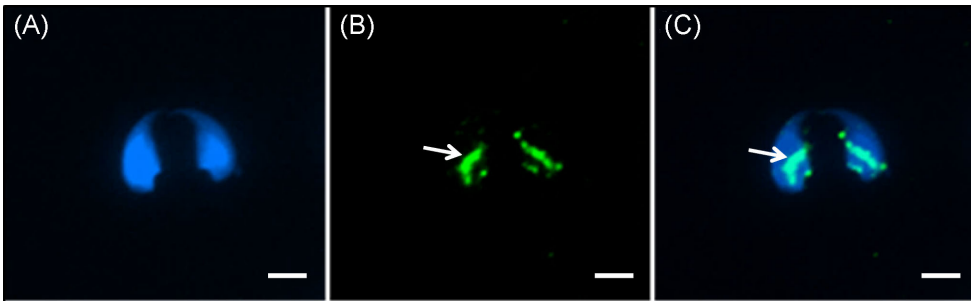

Figure 2. Mouse spermatozoa extracted from vas deferens that were sonicated prior to fixation in 2% formaldehyde, without permeabilization. (A) DAPI alone. (B) Antibody alone. (C) Merge A and B. Note that under these preparatory conditions the PAS (white arrow) is immunoreactive to the antibody but the perforatorium is not labeled. Blue = DAPI, Green = anti-WBP2 (N-14), bar = 5 μm.

Sperm extraction from CD1 mice

Spermatozoa were obtained from the fresh cauda and caput epididymides of sacrificed mature CD1 male mice. The epididymides were placed in 5 ml TBS (pH 7.5–8) solution. The spermatozoa were collected in TBS solution by cutting and gently squeezing the epididymides so that the spermatozoa diffused into the solution. The sperm-containing suspension was aliquoted into four 1.5 ml Eppendorf tubes and washed by centrifugation in TBS twice at 1000 g for 5 min. The sperm pellets were either used immediately or frozen at –80°C until needed.

For immunofluorescence experiments, mature spermatozoa were obtained from the vas deferens, and testicular smears were obtained from the testes of sacrificed mature CD1 male mice. For the extraction of mature sperm, the vas deferens was placed in approximately 2ml of TBS (pH 7.5–8) solution, and sperm were isolated by gently squeezing the vas deferens so that the sperm diffused into the

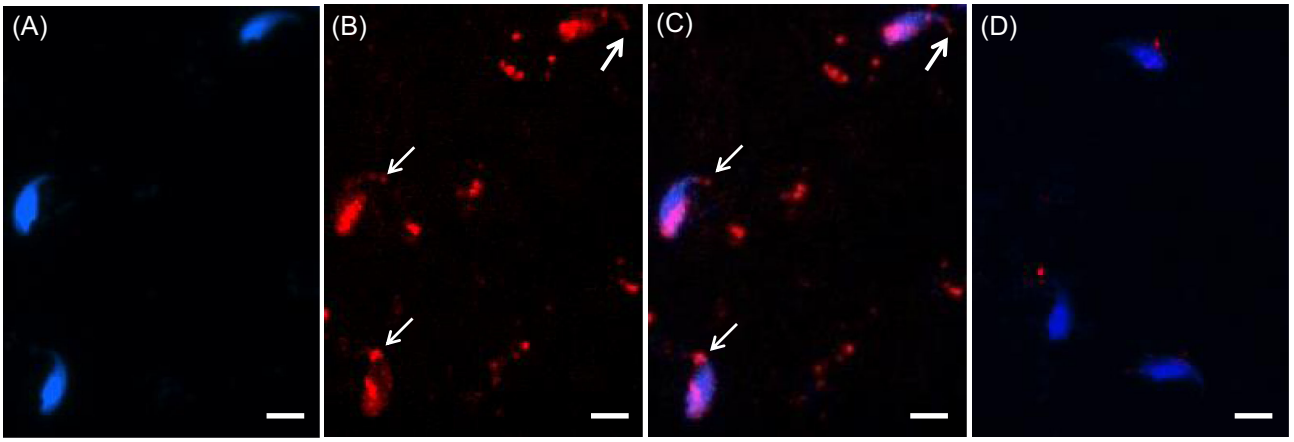

Figure 3. Immunocytochemistry showing specificity of WBP2 labeling in mature mouse spermatozoa. Mouse spermatozoa from the vas deferens were sonicated for 5 s, fixed in 4% paraformaldehyde and permeabilized with Triton-X-100. (A) DAPI alone. (B) Antibody alone. (C) Merge A and B. Note in B and C that with the added permeabilization step the perforatorium became immunoreactive (white arrows) in addition to the PAS (compare with Figure 2). (D) When the anti-WBP2 antibody was pre-incubated with its blocking peptide before primary antibody incubation no labeling was found in the PT regions. Blue = DAPI, Red = anti-WBP2 (N-14), bar = 5 μm.

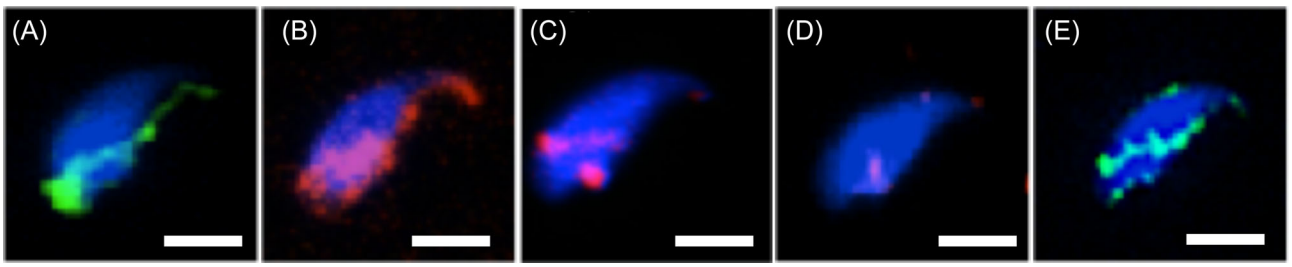

Figure 4. Mouse sonicated sperm showing the labeling pattern of WBP2NL (A) and WBP2 (B) when sonicated for 5 s before fixation and permeabilization. When sonicated for a longer time (3 × 10 s) the amount of WBP2 present is greatly reduced (C) but the labeling pattern remains consistent. If the sonicated sperm heads (SSpH) are treated with 2% Triton-X-100 for 2 h at room temperature before fixation and permeabilization the WBP2 labeling is lost (D) as contrary to WBP2NL, which is retained (E). Blue = DAPI, Red or green = anti-WBP2 (N-14), bar = 5 μm.

solution. The extracted spermatozoa were either used directly or sonicated for 5 s in the presence of PMSF with a small probe Vibra-Cell sonicator (Sonics and Materials) before use. The testicular smears were obtained and processed for immunofluorescence microscopy according to protocols previously published [25]. Briefly, the tunica albuginea was removed from the testes before the testes were placed in 5 ml 200 mM PBS. The testes were cut into smaller pieces using scissors and spermatids were gently squeezed out into the solution from the seminiferous tubules.

Antibodies

The primary antibody used in the experiments was polyclonal goat anti-WBP2 (N-14) (Santa Cruz) at a 1:250 concentration for western blot analysis, and at a 1:30 concentration for immunofluorescence and enzymatic immunohistochemistry. An additional anti-WBP2 primary antibody (ProteinTech, 12030-1-AP, Rosemont, IL) was also used at concentrations recommended by the manufacturer. For western blot analysis, the secondary antibody used was rabbit anti-goat IgG-HRP (horseradish peroxidase) (Santa Cruz, 1:10,000), whereas for immunofluorescence, either donkey anti-goat IgG-CFL (colorized fluorochrome) 555 (Santa Cruz, 1:200) or donkey anti-goat IgG-FITC (fluorescein isothiocyanate) (Santa Cruz, 1:200) was used. The secondary antibody used in enzymatic immunohistochemistry was a biotin labeled rabbit anti-goat IgG(H + L) (Cytodiagnositcs, 1:200). Blocking peptide WBP2 (N-14) P (Santa Cruz) was used at a 2:1 peptide-to-antibody ratio. Polyclonal rabbit serum was raised against human recombinant (r) WBP2NL protein that was produced from WBP2NLcDNA expression vector (pET28a-N-His-Tag) within E. coli host BL21 (DE3). The immune serum was then affinity purified on immobilized His-tag purified rWBP2NL protein and eluted with glycine HCL followed by neutralization with TBS (pH 8) [26].

Western blot analysis

Testicular tissues or sperm samples were solubilized or dissolved, respectively, in reducing sample buffer (200 mM Tris pH 6.8, 4% SDS, 0.1% bromophenol blue, 40% glycerol, 5% β-mercaptoethanol). Approximately 5–10 million spermatozoa were loaded per lane in each experiment and resolved on 4% stacking and 10% separating polyacrylamide gels as described by Laemmli [27] along with a PINK plus prestained protein ladder (GeneDirex). The gel was run at 100 volts for 110 min, and then the proteins were transferred onto a polyvinylidene fluoride (PVDF) membrane (Millipore) for 100 min in Tris-glycine transfer buffer on ice using a Hoefer Transphor apparatus (Hoefer Scientific Instruments). The membrane was blocked with 10% skim milk in phosphate-buffered saline (PBS) with

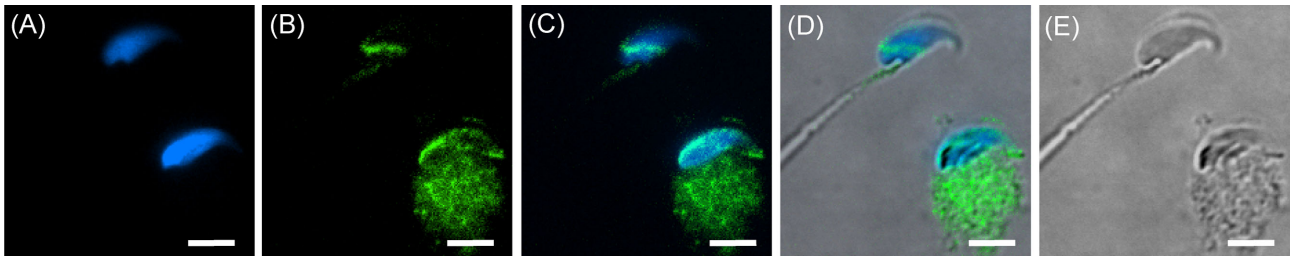

Figure 5. Immunocytochemistry showing the presence of WPB2 in elongating and elongated mouse spermatids fixed with 2% formaldehyde. (A) DAPI alone. (B) Antibody alone. (C) Merge A and B. (D) Merge C with E, which is a differential interference contrast picture of the same field. Note that in the elongated spermatid, at the top of the panel, WBP2 has been incorporated as part of the PAS while in the elongating spermatid, found below, WBP2 is still distributed throughout the cytoplasm lobe. Blue = DAPI, Green = anti-WBP2 (N-14), bar = 5 μm.

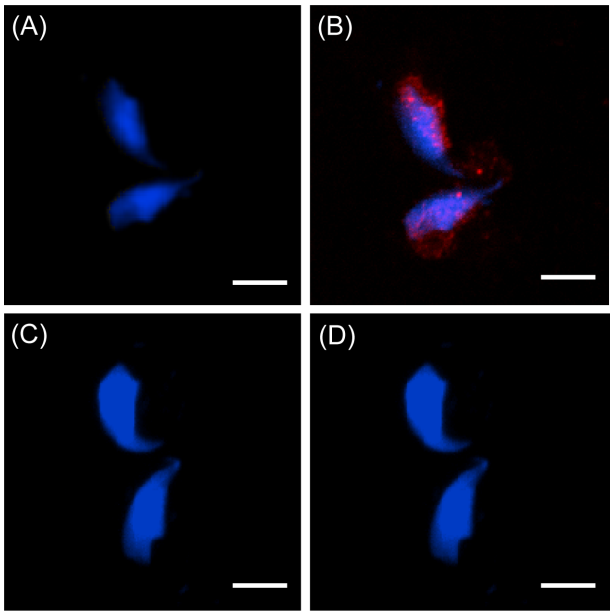

Figure 6. Confirmation that the WBP2 immunoreactivity in the elongating/elongated spermatid cytoplasm is specific. (A) DAPI alone. (B) DAPI plus anti-WBP2 (N-14) antibody labeling. (C) DAPI alone (D) DAPI and anti-WBP2 (N-14) antibody plus its blocking peptide (compare B to D). Blue = DAPI, Red = anti-WBP2 (N-14), bar = 5 μm.

0.05% Tween-20 (PBS-T) for 30 min to avoid nonspecific binding, then incubated with primary antibody overnight at 4°C. The membrane was washed six times in PBS-T for 5 min each and then incubated with secondary antibody conjugated to horseradish peroxidase for 4 h. The membrane was again washed extensively again before the immunodetection reaction was visualized using Clarity Western ECL Substrate (Bio Rad Laboratories). The membrane was then exposed to X-ray film for developing.

WBP2 sperm equivalent estimation

The amount of WBP2 present in a single mouse spermatozoon was estimated based on the densitometric comparison of known concentrations of recombinant WBP2 and known amounts of mouse spermatozoa using anti-WBP2 (ProteinTech) immunoblotting. The immunoreactivity of the bands was analyzed using ImageJ software and a standard curve of recWBP2 plotted using Microsoft Excel. The curve was used to extrapolate the WBP2 protein concentration per single mouse spermatozoon.

Immunofluorescence

Mouse spermatids or spermatozoa were mounted on poly-L lysine coated coverslips and washed with PBS. The cells were then fixed with 4% paraformaldehyde in PBS-T for 40 min at room temperature, and then washed with PBS again. The cells were blocked with 3% bovine serum albumin (BSA) in PBS-T for 25 min to avoid nonspecific binding, and then incubated with primary antibody overnight at 4°C. Next, the cells were washed in PBS and then incubated in secondary antibody conjugated to a fluorescent marker for 40 min at room temperature. The secondary antibody mixture included blue-fluorescence DNA-stain DAPI (4',6-Diamidino-2-Phenylindole, Dihydrochloride). The coverslips were then mounted onto glass slides using para phenylenediamine (PPD) and sealed with nail polish. Images from the slides were captured at Queen's University Cancer Biology Institute Imaging Centre, using a Quorum Wave Effects spinning disc confocal microscope.

Immunohistochemistry

Mouse testicular sections from testes that had been perfusion-fixed in Bouin's fixative and embedded in paraffin were deparaffinized in xylene and hydrated through a graded series of ethanol solutions. During hydration, the sections were treated to abolish endogenous peroxidase activity, to neutralize residual picric acid, and to block free aldehyde groups [28]. Once hydrated, the sections were subjected to antigen retrieval by microwave irradiation in a 0.01 M sodium citrate solution, pH 6 [18]. Immunolabeling was conducted using an avidinbiotin complex (ABC) kit (Vector Laboratories) and followed the procedure outlined by Ferrer et al. [29]

Recombinant WBP2NL and WBP2 proteins and PPXY and PPXA peptides

Recombinant human WBP2NL protein was custom made by GenScript (Piscataway, NJ 08854, USA). The expression product of a WBP2NL-cDNA expression vector (pET28a—N-His-Tag) within mammalian HEK 293 cells was collected and purified on a Ni-affinity column. Purified WBP2NL was visualized on PAGE stained with Coomassie blue and on westerns by immunoblotting with anti-human PAWP antibody.

Recombinant human WW domain binding protein 2 (WBP-2) was purchased from ProSpec (East Brunswick, 08816 NJ; catalogue number PRO-1208). Human and mouse WBP2 sequences are 97% identical. It is important to note that recombinant human WBP2NL protein was expressed in human kidney cells rather than in bacteria in order to obtain it in its folded soluble form. In bacteria WBP2NL would always be packaged into inclusion bodies (pellet) and little

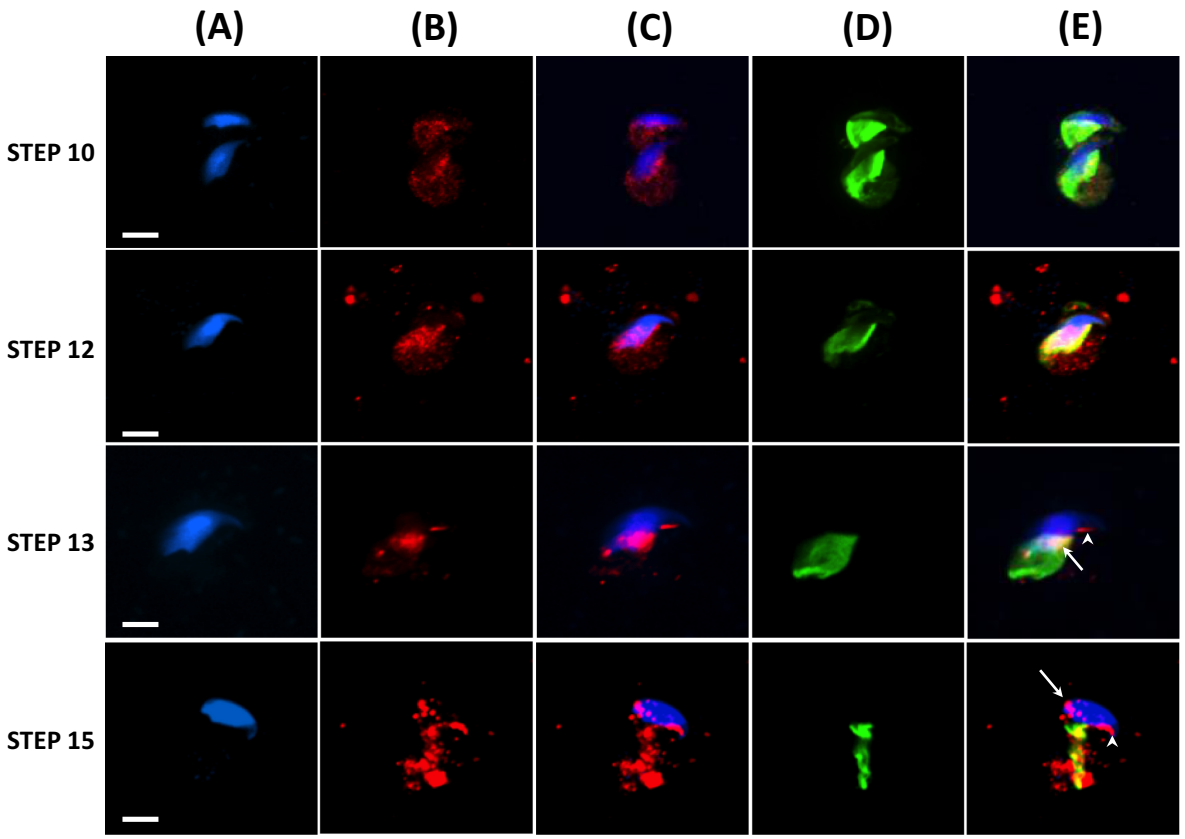

Figure 7. Immunofluorescence showing developmental progression, during the 16 steps of spermiogenesis, in and the association of WBP2 and Tubulin (manchette) in mouse spermatids. Mouse spermatids from testicular extract were fixed in 4% paraformaldehyde and permeabilized after fixation with Triton-X-100. (A) DAPI alone. (B) Anti-WBP2 antibody alone. (C) Merge A and B. (D) Anti-Tubulin antibody alone. (E) C and D merged. Blue = DAPI, Red = anti-WBP2 (N-14), Green = anti-Tubulin, Yellow = the colocalization of WBP2 and Tubulin, Bar = 5 μm.

if any could be obtained directly in its folded soluble form (supernatant). In contrast obtainment of soluble folded WBP2 in bacteria was not an issue. It is also important to note that both WBP2 and WBP2NL are cytosolic proteins and not glycoproteins and thus are not subject to complex post-translational modifications that require a eukaryotic/mammalian cell; however, we cannot exclude at this time whether either or both proteins may require a processing step to become fully active.

PPGY-containing peptide derived from PAWP sequence (Ac-PPVRYGSPPPGYEAPT-CONH2) and its mutant form PPGA (Ac-PPVRYGSPPPGAEAPT-CONH2) were synthesized by DGpeptides CO., Ltd (Hangzhou City, China) at greater than 95% purity.

Mouse gamete preparation, microinjection, and analysis

Mouse cauda epididymides were isolated from young adult BLK-6 males and punctured with a 26G needle to allow spermatozoa to swim out into Embryomax human tubal fluid (HTF) medium (Millipore catalogue number MR-070-D). The spermatozoa were then kept at 37°C and 5%CO_2 until needed. Eight-week-old CD-1 females were superovulated by intraperitoneal injection of 10 IU pregnant mare serum gonadotropin (Sigma) followed 48 h later with 10 IU human chorionic gonadotropin (Sigma). Oocytes were collected from oviducts into M-2 medium (Millipore) 15 h after hCG injection and cumulus oophorus cells removed by treatment with 0.1% hyaluronidase in M-2. The cumulus-free oocytes were washed in M2. Micromanipulation and ICSI were performed according to standard protocols on the stage of a Nikon Ti-S inverted microscope (Nikon Canada Inc., Mississauga, ON, Canada) fitted with Narishige micromanipulators (Narishige International US Inc., Amityville NY, USA) and Piezo PMM-150HJ/FU (Prime tech Ltd, Ibaraki, Japan). Individual spermatozoa, sham control (10 mM PBS microinjection buffer), sham with 0.02 μg/μl BSA, recombinant human WBP2NL (0.0075 μg/μl), and recombinant WBP2 (0.0075 μg/μl) with and without PPXY and PPXA peptides (at concentrations of 0.3 μg/μl) were microinjected to 3–5% of oocyte volume, as estimated from the displacement caused by bolus injections. Based on this percentage and our concentration of recombinant (0.0075 μg/μl) we estimate that only 5 pl of our recombinant solution was delivered safely. The amount of protein in 5 pl of 0.0075 μg/μl is 0.0375 pg which is well below the estimated bull sperm equivalent [19] of 0.08 μg/μl of WBP2NL. Oocytes were incubated at 37°C, 5% CO2 for 9–10 h after injection. They were subsequently fixed in 2% formaldehyde and stained with DAPI (0.3 mg/ml) or Hoescht (1 μg/μl) and imaged using a Quorum Wave Effects Spinning Disc Confocal microscope.

Statistics

A Chi-squared test was performed between experimental groups and the negative control to determine statistical significance. Standard error was determined and statistical significance was noted when $P < 0.05$.

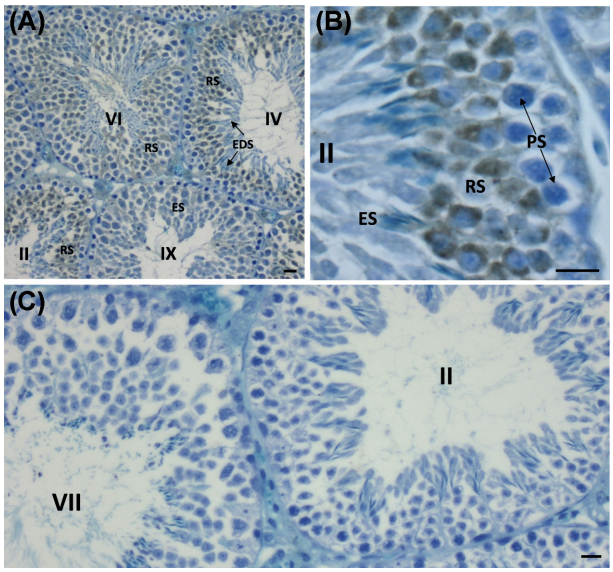

Figure 8. Immunoperoxidase labeling of the mouse seminiferous epithelium with anti-WBP2 (N-14) antibody. Stages of the 12 stage cycle of the mouse seminiferous epithelium are marked by Roman numerals. (A) Low magnification section through mouse seminiferous tubules labeled with anti-WBP2 antibody. Note that the round spermatids (RS) are intensely immunoreactive. (B) Higher magnification of seminiferous epithelium in stage II showing relatively intense immunoreactivity in the cytoplasm of round spermatids compared to elongating spermatids (ES) in step 14 of spermiogenesis and pachytene spematocytes (PS). (C) When the anti-WBP2 antibody was preincubated with its blocking peptide before primary antibody incubation no labeling was found anywhere throughout the seminiferous epithelium. Bar in A = 20 μm, Bars in B and C = 10 μm.

Results

The presence of WBP2 in the testis and sperm of eutherian mammals

Western blot analysis performed with polyclonal goat anti-WBP2 labeled a band at approximately 40 kDa in the mouse, human and bull testes (Figure 1A). The mouse sperm sample also labeled a band at this level, yet it appeared absent in both human and bull sperm. An additional western blot was also performed to compare the presence of WBP2 in spermatozoa of multiple mammalian species (Figure 1B). An immunoreactive band was present at 40 kDa in mouse and rat spermatozoa but was absent from boar, human and bull spermatozoa. This pattern of labeling suggests that WBP2 is present in the testis of nonmurid eutherian mammals but not necessarily in their spermatozoa. To confirm the specificity of the anti-WBP2(N-14) antibody, it was preincubated with WBP2(N-14) blocking peptide prior to primary antibody incubation on western blots of mouse testicular and sperm samples (Figure 1C). Bands at 40 kDa were present in the mouse testis, sperm and HeLa cells (not shown), however, with the WBP2 (N-14) blocking peptide, the 40 kDa bands disappeared, indicating that the 40 kDa band is specific to WBP2. It should be noted that in the mouse spermatozoa an immunoreactive band slightly higher than the 40 kDa level was resistant to the block along with two more nonspecific bands with much higher molecular masses.

In order to confirm that WBP2 is not just a surface component of mouse spermatozoa, washed sperm pellets were resuspended in TBS and sonicated for 5 s to disrupt and separate the plasma membrane, the outer acrosomal membrane and the contents of the acrosome from the sperm. The resulting supernatant, presumably containing these disrupted sperm components, and pellet obtained from high speed centrifugation of this sonicated sperm solution were then compared for the relative amounts of WBP2 in each fraction (Figure 1D). Western blots revealed a relatively stronger WBP2 immunoreative band in the SDS extract of the pellet than in the supernatant, indicating that WBP2 is an internal component of the mouse sperm, although not excluding that it could be a surface component as well.

To indirectly test the degree of WBP2 binding to internal sperm structures, mouse spermatozoa were successively extracted in nonionic (NP-40) and ionic detergents (SDS), with washes of the centrifuged sperm pellets in between. Interestingly, Western blot comparison of the two extracts revealed that WBP2 was completely extractable from mouse spermatozoa in nonionic detergents (Figure 1E), suggesting that WBP2 weakly interacts with internal sperm structures. Finally, to test that the antibodies raised against WBP2 and WBP2NL were not detecting common antigenic epitopes between these two paralogs, the immunolabeling patterns of anti-WBP2 (N14) and anti-WBP2NL on westerns of identical mouse sperm extracts were compared (Figure 1F). Anti-WBP2 (N-14) antibody only recognized a protein band in the supernatant of the sperm NP40 extract but not in the pellet, while anti-WBP2NL only recognized a similar sized band in the pellet of the NP40 extracted sperm but not in the supernatant. The resistance of WBP2NL to extraction from the sperm in nonionic detergent was expected [11].

Localization of WBP2 in mouse sperm

To find the location(s) of WBP2 in mouse sperm, immunofluorescence and confocal microscopy utilizing the anti-WBP2 (N-14) antibody was first performed on sonicated mouse spermatozoa that were fixed in paraformaldehyde but nonpermeabilized. The immunolabeling was found over the postacrosomal region of the sperm heads (Figure 2). However, if the fixed spermatozoa were permeabilized before immunolabeling, both the postacrosomal and perforatorial regions of the PT were labeled (Figure 3A–C). When the antibody was preincubated with the peptide it was raised against (N-14) (Figure 3D) or substituted with goat IgG (Figure 3E), both regions of the PT remained unlabeled, confirming the specificity of the antibody.

To compare the positioning and relative degree of WBP2- and WBP2NL-binding in the PT, mouse spermatozoa were subjected to increasing lengths of sonication followed by a final extraction in nonionic detergent. After a 5 s sonication burst both WBP2 and WBP2NL were strongly immunolabeled over the postacrosomal and perforatorial regions of the PT (Figure 4A and B). However, after a prolonged bout of sonication, which breaks the apical tip of the perforatorium off the sperm head, only a relatively moderate level of WBP2 immunoreactivity remained in the postacrosomal region of the sperm head (Figure 4C). Moreover, on subsequent nonionic detergent extraction of the sonicated spermatozoa, the WBP2 immunolabeling completely disappeared in the PAS in contrast to the retention of WBP2NL labeling in this region (compare Figure 4D and E). This corroborates our western blot results showing that nonionic detergent incubation is sufficient to eliminate most of the WBP2 from the sperm head. It also shows that compared to WBP2NL, WBP2 is less firmly bound to the PT.

Localization of WBP2 in mouse testis

To find out if WBP2 shares a similar pattern of expression and PT assembly during spermiogenesis with previously characterized PAS proteins, mouse testicular germ cell smears were evaluated for localization of WBP2 by immunofluorescence. As shown for other PAS

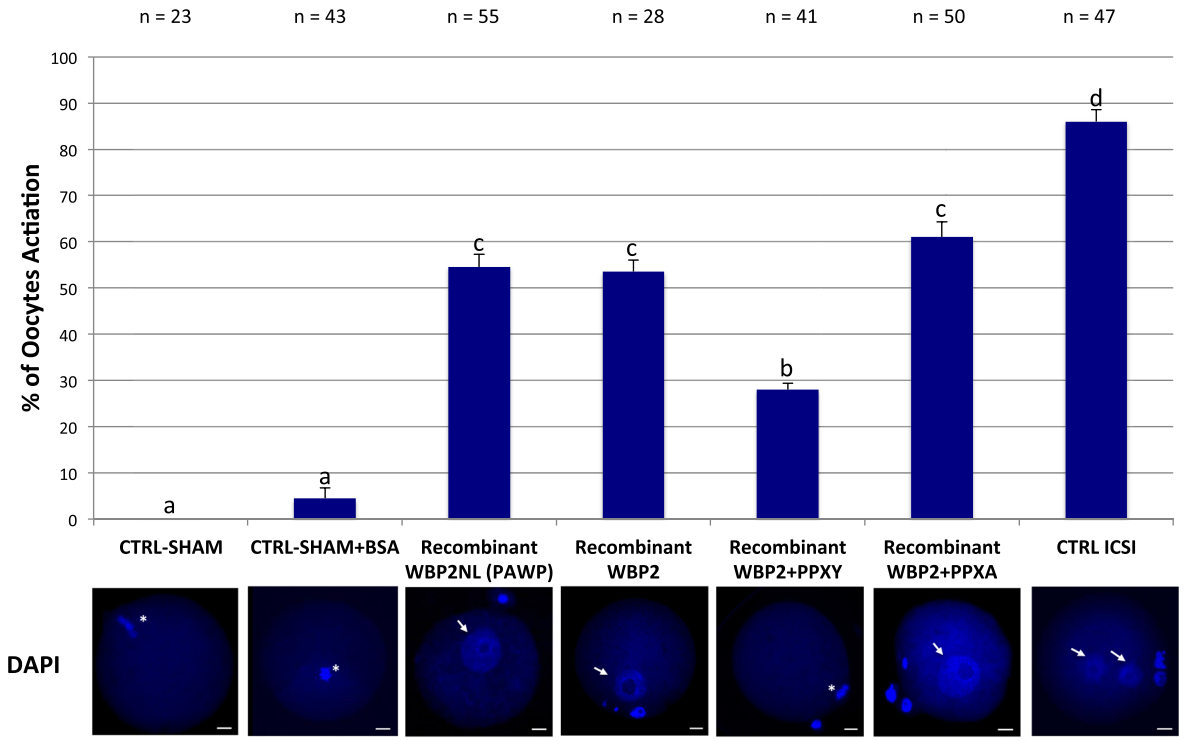

Figure 9. Comparison of mouse oocyte activation rates between sham, sham + BSA, recombinant (r)WBP2NL (PAWP), rWBP2, rWBP2 + PPXY, rWBP2 + PPXA and sperm heads (CTRL ICSI) 9–10 h after microinjection into metaphase II arrested oocytes (three or more replicates were done for each experimental group except for sham (without BSA) where only 2 replicates were done). In the positive control (ICSI), metaphase II arrested oocytes that were injected with sperm heads had an average activation rate of 86%, based on the formation of male and female pronuclei. Recombinant WBP2NL (0.0075 μg/μl) and rWBP2 (0.0075 μg/μl) injections produced average activation rates over 50%, based on the formation of a female pronucleus. Coinjection of PPXY peptide with rWBP2 significantly reduced the activation rate obtained with rWBP2 alone, while coinjection PPXA peptide with rWBP2 had no significant effect. The negative control, sham + BSA, had a 4% activation rate with most oocytes remaining arrested in metaphase II while sham had a 0% activation rate. Representative DAPI stained images of pronuclei progression within oocytes or ova for respective microinjection regime are found directly below bar graphs. Pronuclei, arrows; metaphase II plate, asterisk; bar = 20 μm. Superscript letters (a, b, c) indicate significant differences at $P < 0.05$ and error bars denote standard error.

proteins [16, 18], WBP2 is distributed throughout the cytoplasmic lobe of elongating spermatids before it assembles as part of the PAS at the end of elongation (Figure 5). The specificity of the cytoplasmic immuno-labeling was confirmed by incubating the anti-WBP2 (N-14) antibody with WBP2 (N-14) blocking peptide prior to labeling the spermatids with the antibody (Figure 6).

Because most PAS proteins, that have been developmentally characterized, are transported by the microtubules of the manchette to their site of assembly on the spermatid head [16, 18] we addressed whether WBP2 uses this route as well. Indeed, we confirmed that this is the most likely transport route for WBP2 by showing the close association of WBP2 and tubulin on the manchette by immunofluorescent colocalization (Figure 7). The association of WBP2 with the microtubules of the manchette begins early in the spermatid elongation phase, suggesting that a portion of this protein, once synthesized in the cytoplasmic lobe, is stored on this apparatus until its assembly as part of the PAS (Figure 7, Step 10). In fact, towards the end of nuclear condensation and elongation, a step before the manchette begins to migrate down the caudal half of the spermatid head, the amount of WBP2 associated with the microtubules of the manchette appeared to reach a peak (Figure 7, Step 12). In step 13, the manchette begun its migration down the caudal half of spermatid head and both the PAS (arrow) and perforatorium (arrowhead) appear to form in its wake (Figure 7, Step 13). By step 15, the manchette had migrated off the spermatid head leaving behind the assembled PAS (arrow) and perforatorium (arrowhead) (Figure 7, Step 15). These findings suggest that WBP2 initially associates with the microtubules of the manchette in the elongation phase of spermiogenesis and then is transported to its place of assembly in both the postacrosomal and perforatorial regions of the sperm head in the wake of the descending manchette.

Surprisingly, immunohistochemistry of the testes revealed that WBP2 was much more concentrated throughout the cytoplasm of round spermatids than in the cytoplasm of the elongating spermatids (Figure 8).

Oocyte-activating ability of WBP2 as compared to WBP2NL

Because WBP2 has a similar distribution in mouse sperm as WBP2NL and also displays similar motifs, we compared the oocyte-activating ability of recombinant WBP2 and WBP2NL. Super-ovulated metaphase II arrested oocytes were microinjected by a piezo-driven system with injection buffer (10 mM PBS, sham), sham containing 0.02 μg/μl of BSA (sham BSA), human recombinant WBP2NL (0.0075 μg/μl) or human recombinant WBP2 (0.0075 μg/μl) with and without PPXY and PPXA peptides (at concentrations of 0.3 μg/μl) and the oocyte activation outcome compared by assessing

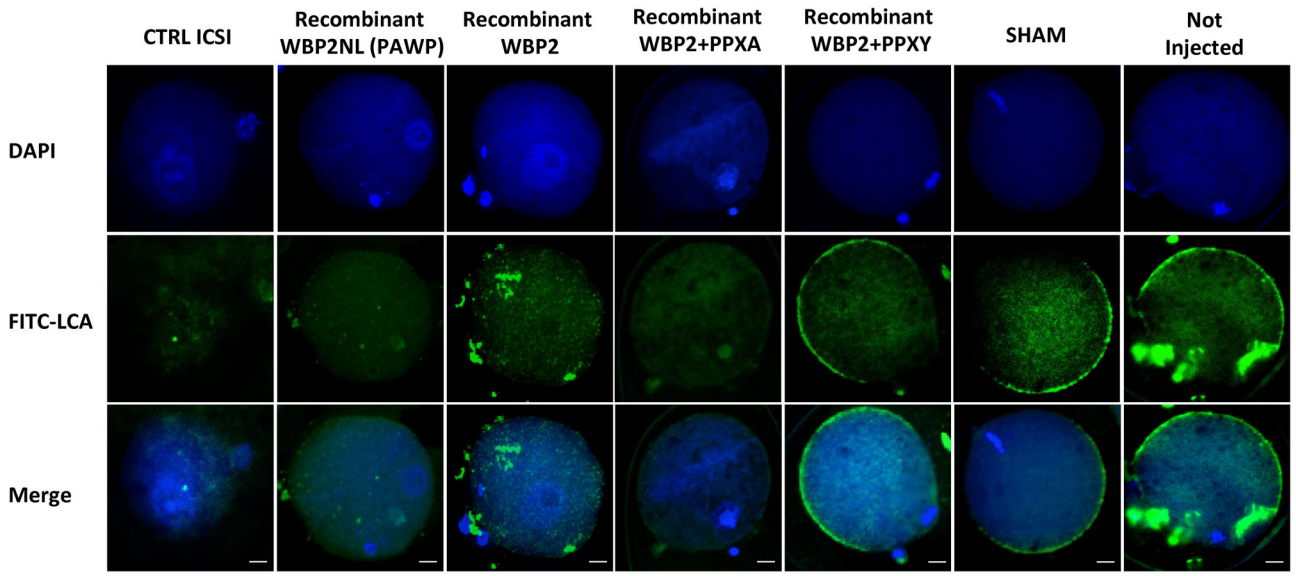

Figure 10. Cortical granule exocytosis in rWBP2NL and rWBP2 microinjected mouse oocytes that display pronuclear formation. The pronuclear development in each treatment group was evaluated through nuclear staining (DAPI). The cortical granule exocytosis reaction was assessed through staining with FITC conjugated LCA (FITC-LCA) and both DAPI and FITC-LCA staining were overlaid to show the correlating trends in staining patterns when oocytes were and were not activated (Merge). Bar = 20 μm

the presence of a fully formed female pronucleus, 9–10 h after injection. Sperm injected metaphase II oocytes were used as a positive control. Sham injected negative controls had no activation and sham negative controls that included additional BSA as a protein control activated 4% of the oocytes. In contrast, sperm injected positive controls activated 86% of the oocytes while recombinant WBP2NL and WBP2 activated over 50% of the oocytes injected (Figure 9). The PPXY peptide significantly inhibited the activation rate of WBP2 while its mutant PPXA had no effect. Oocytes that maintained the MII plate and did not progress developmentally showed a strong staining around their perimeter with FITC-LCA suggesting the cortical granule exocytosis reaction had not occurred (i.e. Recombinant WBP2 + PPXY, SHAM and Not Injected). In contrast, oocytes that had formed prouclei at 9–10 h had lost the FITC-LCA staining signifying the cortical granules had been released (i.e. CTRL ICSI, Recombinant WBP2NL, Recombinant WBP2 and Recombinant WBP2 + PPXA) (Figure 10).

Discussion

This study was done on the premise that WBP2 can compensate for a WBP2NL deficiency in oocyte activation. A mouse *Wbp2nl* gene KO showed that mice remain fertile [24] even though earlier studies predicted that WBP2NL was required for fertilization on the basis that (ICSI)- or WBP2NL protein-induced oocyte activation was blocked by a competitive inhibitor derived from a PPXY motif of WBP2NL [19, 22, 23]. Since WBP2 is WBP2NL's precursor, contains PPXY motifs and its mRNA is expressed in the testis [30], the intention of this study was to provide further support for its candidacy as a SOAF in mouse that could compensate for a deficiency in WBP2NL. For WBP2 to meet the criteria of a SOAF it must be a sperm head component that most likely is found in the postacrosomal region of the PT. Additionally, it is most likely expressed in the latter half of spermiogenesis during spermatid elongation and assembled as part of the PAS-PT at the end of spermatid nuclear condensation and elongation. In this study we provide the evidence to show that WBP2 meets these locational and developmental requirements of a SOAF.

A conscious effort was made in our analyses to coordinate our western blot analysis of successive sperm extractions (i.e. sonication, nonionic detergents and ionic detergents) with the consequence on the fluorescent labeling of WBP2. Once we were convinced that WBP2 was a component of mouse sperm head, we addressed the issue of whether it was a surface component by sonication to remove the sperm plasmalemma and disrupt the acrosome. Both western blot and immuno-fluorescent labeling analyses showed that a substantial amount of WBP2 was retained within the sperm on the PAS-PT after sonication. Surprisingly, if the sonicated spermatozoa were membrane permeabilized an additional immuno-fluorescent labeling of WBP2 was found over the perforatorium. Most likely this added consequence of permeabilization was due to perforating the inner acrosomal membrane, which is retained after sonication and overlays the perforatorium. We then addressed the relative strengths of WBP2 and WBP2NL binding interactions with the PAS-PT and perforatorium by increasing the intensity of sonication and comparing their extractability in various detergents. Although there appeared to be an incremental extractability of WBP2, but not of WBP2NL, with increasing sonication intensity, a portion of WBP2 was still retained in the PAS. However, as substantiated by both western blotting and immunofluorescence, sperm extractions in nonionic detergents (i.e. NP-40 or Triton X-100) completely removed WBP2 from both the PAS and perforatorium but were unable to extract WBP2NL. The WBP2 protein therefore appears to be the exception to the rule that the PT is a nonionic detergent resistant protein capsule [11, 13]. If WBP2 proves to be a SOAF component in the mouse, an advantage of being a more readily soluble PT molecule would be a quicker release and hence initiation of the fertilization process after gamete membrane fusion. It is important to note that of the two WBP2 isoforms documented in GenBank our immunoblotting analysis has identified the longer 40kDa form

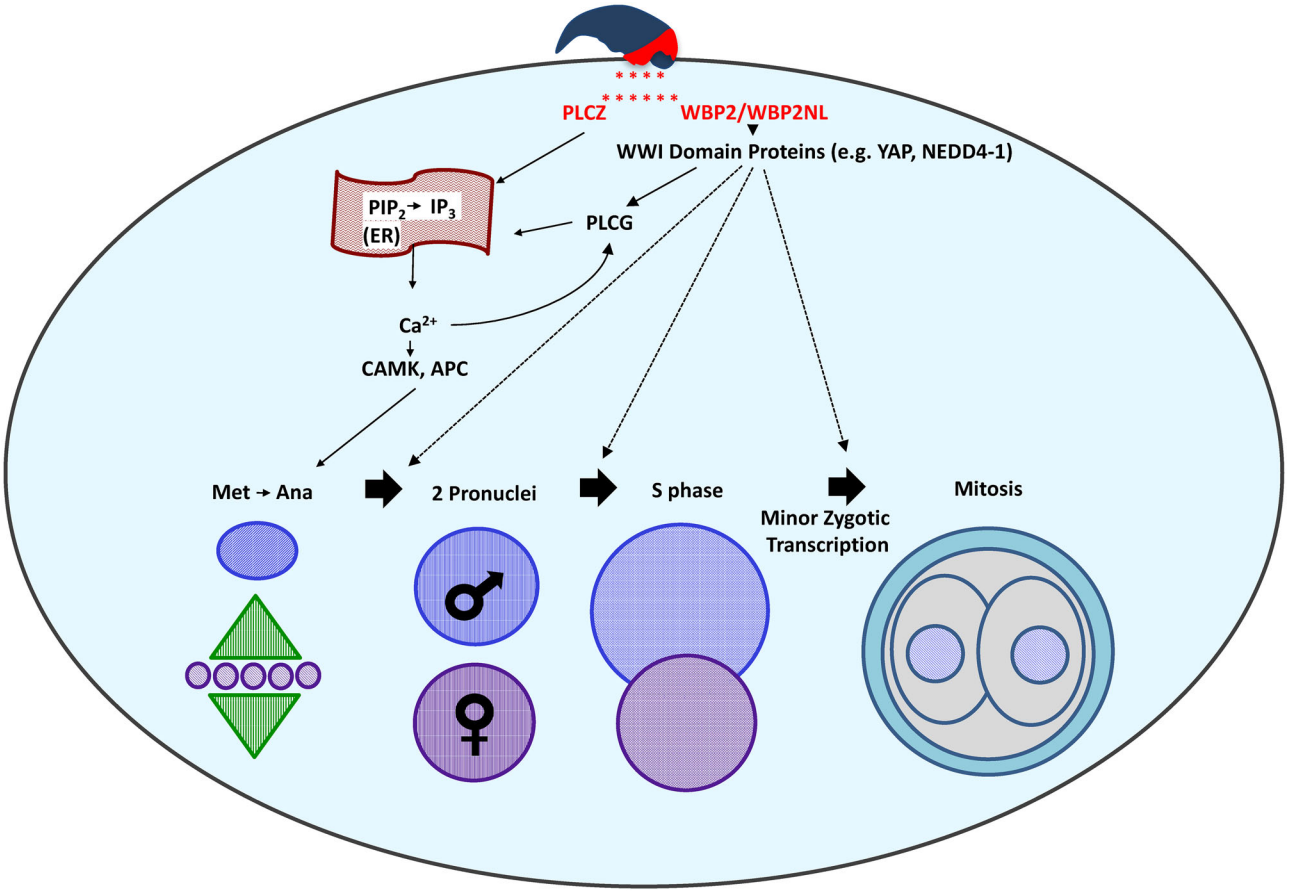

Figure 11. Proposed two-factor mechanism of sperm-induced oocyte activation. The sperm oocyte-activating factor (SOAF) is released from the PAS region of the sperm head PT into the ooplasm upon sperm–oocyte fusion. The two candidate SOAF proteins, PLCZ1 and WBP2NL/WBP2 would facilitate the hydrolysis of PIP_2 to IP_3. Next, IP_3 would bind to the IP_3R receptor on the endoplasmic reticulum (ER), and trigger the release of Ca^{2+} from its stores, ultimately increasing the intracellular Ca^{2+} in the oocyte cytosol. This mechanism would be activated either directly, in the case of PLCZ1, or indirectly in the case of WBP2NL/WBP2. It is proposed that WBP2NL/WBP2 would bind to the ooplasmic WWI domain containing proteins to activate oocyte PLC Gamma (PLCG), catalyzing the hydrolysis of PIP_2 to IP_3. The increase in Ca^{2+} would result in the downstream activation of enzymes such as the calcium-calmodulin kinase (CAMK) and the anaphase promoting complex (APC) catalyzing the completion of oocyte meiosis and further, repetitive Ca^{2+}-induced Ca^{2+} release (Ca^{2+} oscillations). Additionally, WBP2NL/WBP2 may aid in the regulation and/or activation of WWI domain containing proteins shown to have roles in the early stages of zygotic development after the initial activation of the oocyte. Specifically, WBP2/WBP2NL could serve as adaptors of yet to be identified transcription factors responsible for the minor zygotic genome activation, resulting in transcription of a small number of genes in the pronuclei, observed in mammalian zygotes.

(BAB23594.1), which dominates in the testis and sperm in contrast to the shorter WBP2 isoform (NP_058548.1) that prevails in the brain.

As expected of PAS localized proteins [16, 18], WBP2 was found associated with the microtubules of the manchette within the distal mouse spermatid cytoplasm during the elongation phase of spermiogenesis. PAS proteins normally assemble to form the definitive PAS towards the end of the spermatid elongation phase, commensurate with the caudal descent of the manchette [16, 18]. Before its descent the manchette surrounds the spermatid nucleus just below the acrosome in the form of a "microtubular girdle like" structure [11, 31–33]. The distal region of the manchette reaches far into the cytoplasm of the spermatid tail (or cytoplasmic lobe), where PAS proteins including WBP2 are synthesized. A cytoplasmic channel surrounding the nucleus forms from the positioning of the manchette and is filled with microtubules that connect the spermatid nucleus with the cytoplasmic lobe. This positioning combined with the colocalization of PAS proteins on the microtubules implies that the manchette is an important shuttle that conveys PAS proteins from the cytoplasmic lobe to the caudal half of the spermatid head [16, 18] by a process termed intramanchette transport (IMT) [33–37]. The discovery that molecular motor proteins, kinesins and dyneins, are associated with the manchette lends support to this hypothesis [35, 38–40]. The fact that the PAS assembles around the caudal half of the spermatid nucleus in the wake of the descending manchette suggests that the PAS proteins, which are delivered to the space around the nucleus left vacant by the manchette, self-assemble to form the definitive PAS structure. In bovine spermiogenesis the descent of the manchette and assembly of the PAS occurs between steps 11 and 12 [31, 33], while in mouse it occurs between steps 13 and 14 [16].

A novel finding from the present study was that both WBP2 and WBP2NL were found to reside in the perforatorium in mouse and rat spermatozoa (for rat see Supplementary Figure S2), in addition to being components of the PAS-PT where they are expected to reside. It should be noted that the perforatorium does not appear in spatulate shaped eutherian spermatozoa [41]. The perforatorial

localization of these candidate SOAFs is not surprising as a triangular subacrosomal space, which eventually accommodates the perforatorial proteins, forms during the elongation phase of spermatid head development at the time of PAS formation [42]. In fact PERF15, the most prominent perforatorial protein, begins to occupy the subacrosomal space towards the end of spermatid elongation and is also associated with the manchette at this time [43–45]. It is likely that the transportation and deposition of proteins by the manchette in the perforatorial region happens in tandem with the deposition of proteins in the PAS region of the PT. Interestingly, the perforatorial proteins that occupy the triangular subacrosomal space do not condense to form a definitive electron dense perforatorial structure until the last steps of spermiogenesis [33, 42]. Possible advantages of housing SOAF in the perforatorium, in addition to the PAS of murid spermatozoa, are that it may insure an even distribution of this factor throughout the relatively long and oddly shaped falciform head structure and an extra storage facility to assure slow and steady release and thus a longer maintenance of Ca^{2+} oscillations throughout the lengthy process of oocyte activation.

The ability of WBP2 to initiate the same oocyte activation response, as WBP2NL/PAWP is not surprising considering that *Wbp2nl* arose from duplication of *Wbp2* gene (Ensembl: GeneTree ENSGT530000063718). The N-terminal halves of their protein products share high sequence homology and contain a Pleckstrin homology domain shown in other proteins to be involved in membrane-coupling via phosphoinositides. In the C-terminal half, there is little sequence homology between these proteins except for a high proline content and common occurrence of PPXY motifs. Because sperm-, recombinant WBP2NL-, WBP2NL cRNA-, or PT extract-induced oocyte activation is blocked by coinjection of a synthetic peptide derived from PPXY motif of WBP2NL [19, 22, 23] it follows that PPXY motifs in WBP2 also most likely bind to a WW1 domain oocyte containing protein(s) to initiate the cell signaling interaction leading to oocyte activation. The implication that WBP2 initiates its oocyte activation effect through WW1 modular interactions, just as WBP2NL does, is supported by the competitive inhibiting effect of PPXY on the rWBP2-induced oocyte activation rate in this study. Among the potential WW1 containing substrates of the sperm-released WBPs in the ooplasm are the YES-kinase associated protein (YAP), the WW-domain containing ubiquitin ligases HECW1 (NEDL1) and HECW2 (NEDL2) [13] and NEDD4-1 which promotes the targeting of Ca_v channels directly from the ER-Golgi network toward the proteasomal and lysosomal compartments [46]. Because the sperm equivalent of WBP2 in mouse was estimated to be approximately 40x less than found for WBP2NL, WBP2 most likely would have to be developmentally upregulated in order to completely substitute for the oocyte-activating ability of WBP2NL if its gene was ablated.

The mechanisms responsible for oocyte activation are still not fully understood. A recent paper indicates that mouse sperm lacking PLCZ1 fail to trigger Ca^{2+} oscillations in mouse oocyte but that *Plcz1*$^{-/-}$ male mice remain subfertile [4] implying that there is either a delay or change in the calcium response or alternative pathways of oocyte activation in the mouse are operable. Both WBP2NL and WBP2 through their WW1 modular interactions could represent alternative pathways of oocyte activation, which need further investigation. However, this current study showed that cortical granule exocytosis, a downstream event of calcium release, occurred consistently after recombinant WBP2 and WBP2NL injection into mouse oocytes. Thus, a two-factor mechanism of sperm-induced oocyte activation is considered in Figure 11.

We detected WBP2 in mouse and rat spermatozoa, but not in the human or bull spermatozoa. This may be significant because the WBP2NL knockout was only performed in mice [24], thus perhaps WBP2 is only able to compensate for a lack of WBP2NL in mice and other murids. Accordingly, it would be interesting to assess whether other mammals, such as bull or boar, would show a sub-fertile or infertile phenotype if their *Wbp2nl* genes were knocked out. Our study shows that WBP2 shares the same locational and developmental criteria of a SOAF, shares PPXY motifs and a pleckstrin homology domain with WBP2NL, is capable of activating mouse oocytes and importantly is the testicular protein from which WBP2NL originated. Based on this assessement it would be expediant to perform a double gene knockout of *Wbp2nl* and *Wbp2* in mice in order to investigate if WBP2 can really compensate for the a lack of WBP2NL. Furthermore, since the longer isoform of WBP2 resides in the testis/spermatids of a variety of mammals and the *Wbp2nl/Pawp gene* evolved from *Wbp2* when vertebrates first appeared (see http://www.ensembl.org/Multi/GeneTree/Image?gt=ENSGT00530000063718), the possibility exists that a WBP2 isoform was an original testis/sperm specific SOAF in invertebrates.

Supplementary data

Supplementary data are available at *BIOLRE* online.

Supplementary Figure S1. Sequence comparison between WBP2 and WBP2NL. The underlined sequence of 50 aa denotes the region from which the 16 aa peptide was derived to raise the goat anti-WBP2 (N14) antibody used in this study. Potential PPXY motifs are bolded.

Supplementary Figure S2. Rat Whole Spermatozoa WBP2 labeling. (A) The nuclear staining of rat spermatozoa with DAPI. (B) The positive WBP2 labeling in rat spermatozoa, showing reactivity in the PAS and perforatorial regions. (C) A merge of the nuclear staining (A) and WBP2 staining (B). (D) The negative control using Goat IgG showing no nonspecific reactivity of the secondary antibody.

Acknowledgments

We are indebted to Dr Bruce Murphy (Centre de recherche en reproduction fertilité, Faculté de médecine vétérinaire, Université de Montréal) for providing us with the use of the Centre ICSI facility and arranging the expertise and help needed from staff and student members to succeed in our quest. We are particularly grateful to Vickie Roussel for her advice and extra preparatory hours invested in this project. We acknowledge the assistance of Brianna Cameron on this project during her undergraduate studies. We would also like to express our appreciation to Matt Gordon and Jeff Mewburn of the Queen's University Biomedical Imaging Centre for their guidance and assistance in image acquisition and analysis.

References

1. Stice SL, Robl JM. Activation of mammalian oocytes by a factor obtained from rabbit sperm. *Mol Reprod Dev* 1990; **25**:272–280.
2. Swann K. A cytosolic sperm factor stimulates repetitive calcium increases and mimics fertilization in hamster eggs. *Development* 1990; **110**:1295–1302.
3. Swann K, Lai FA. Egg activation at fertilization by a soluble sperm protein. *Physiol Rev* 2016; **96**:127–149.
4. Hachem A, Godwin J, Ruas M, Lee HC, Ferrer BM, Ardestani G, Bassett A, Fox S, Navarrete F, de SP, Heindryckx B, Fissore R et al. PLCzeta is the physiological trigger of the Ca_{2+} oscillations that induce embryogenesis

in mammals but conception can occur in its absence. *Development* 2017; **144**:2914–2924.
5. Kimura Y, Yanagimachi R, Kuretake S, Bortkiewicz H, Perry AC, Yanagimachi H. Analysis of mouse oocyte activation suggests the involvement of sperm perinuclear material. *Biol Reprod* 1998; **58**: 1407–1415.
6. Kuretake S, Kimura Y, Hoshi K, Yanagimachi R. Fertilization and development of mouse oocytes injected with isolated sperm heads. *Biol Reprod* 1996; **55**:789–795.
7. Morozumi K, Shikano T, Miyazaki S, Yanagimachi R. Simultaneous removal of sperm plasma membrane and acrosome before intracytoplasmic sperm injection improves oocyte activation/embryonic development. *Proc Natl Acad Sci* 2006; **103**:17661–17666.
8. Perry AC, Wakayama T, Yanagimachi R. A novel trans-complementation assay suggests full mammalian oocyte activation is coordinately initiated by multiple, submembrane sperm components. *Biol Reprod* 1999; **60**:747–755.
9. Perry AC, Wakayama T, Cooke IM, Yanagimachi R. Mammalian oocyte activation by the synergistic action of discrete sperm head components: induction of calcium transients and involvement of proteolysis. *Dev Biol* 2000; **217**:386–393.
10. Tran MH, Aul RB, Xu W, van der Hoorn FA, Oko R. Involvement of classical bipartite/karyopherin nuclear import pathway components in acrosomal trafficking and assembly during bovine and murid spermiogenesis. *Biol Reprod* 2012; **86**:84.
11. Oko R, Sutovsky P. Biogenesis of sperm perinuclear theca and its role in sperm functional competence and fertilization. *J Reprod Immunol* 2009; **83**:2–7.
12. Ferrer M, Xu W, Oko R. The composition, protein genesis and significance of the inner acrosomal membrane of eutherian sperm. *Cell Tissue Res* 2012; **349**:733–748.
13. Oko R, Aarabi M, Mao J, Balakier H, Sutovsky P. Sperm specific WW-domain binding proteins. In: DeJonge C, Barrat C (eds.), *The Sperm Cell: Production, Maturation, Fertilization, Regeneration*, Second Edition ed. Cambridge, UK: Cambridge University Press; 2017: 157–176.
14. Sutovsky P, Manandhar G, Wu A, Oko R. Interactions of sperm perinuclear theca with the oocyte: implications for oocyte activation, antipolyspermy defense, and assisted reproduction. *Microsc Res Tech* 2003; **61**:362–378.
15. van der Spoel AC, Jeyakumar M, Butters TD, Charlton HM, Moore HD, Dwek RA, Platt FM. Reversible infertility in male mice after oral administration of alkylated imino sugars: a nonhormonal approach to male contraception. *Proc Natl Acad Sci USA* 2002; **99**: 17173–17178.
16. Wu AT, Sutovsky P, Xu W, van der Spoel AC, Platt FM, Oko R. The postacrosomal assembly of sperm head protein, PAWP, is independent of acrosome formation and dependent on microtubular manchette transport. *Dev Biol* 2007; **312**:471–483.
17. Suganuma R, Walden CM, Butters TD, Platt FM, Dwek RA, Yanagimachi R, van der Spoel AC. Alkylated imino sugars, reversible male infertility-inducing agents, do not affect the genetic integrity of male mouse germ cells during short-term treatment despite induction of sperm deformities. *Biol Reprod* 2005; **72**:805–813.
18. Tovich PR, Sutovsky P, Oko RJ. Novel aspect of perinuclear theca assembly revealed by immunolocalization of non-nuclear somatic histones during bovine spermiogenesis. *Biol Reprod* 2004; **71**:1182–1194.
19. Wu AT, Sutovsky P, Manandhar G, Xu W, Katayama M, Day BN, Park KW, Yi YJ, Xi YW, Prather RS, Oko R. PAWP, a sperm-specific WW domain-binding protein, promotes meiotic resumption and pronuclear development during fertilization. *J Biol Chem* 2007; **282**:12164–12175.
20. Kay BK, Williamson MP, Sudol M. The importance of being proline: the interaction of proline-rich motifs in signaling proteins with their cognate domains. *FASEB J* 2000; **14**:231–241.
21. Macias MJ, Wiesner S, Sudol M. WW and SH3 domains, two different scaffolds to recognize proline-rich ligands. *FEBS Lett* 2002; **513**:30–37.
22. Aarabi M, Qin Z, Xu W, Mewburn J, Oko R. Sperm-borne protein, PAWP, initiates zygotic development in Xenopus laevis by eliciting intracellular calcium release. *Mol Reprod Dev* 2010; **77**:249–256.
23. Aarabi M, Balakier H, Bashar S, Moskovtsev SI, Sutovsky P, Librach CL, Oko R. Sperm-derived WW domain-binding protein, PAWP, elicits calcium oscillations and oocyte activation in humans and mice. *FASEB J* 2014; **28**:4434–4440.
24. Satouh Y, Nozawa K, Ikawa M. Sperm postacrosomal WW domain-binding protein is not required for mouse egg activation. *Biol Reprod* 2015; **93**:94.
25. Sutovsky P, Ramalho-Santos J, Moreno RD, Oko R, Hewitson L, Schatten G. On-stage selection of single round spermatids using a vital, mitochondrion-specific fluorescent probe MitoTracker(TM) and high resolution differential interference contrast microscopy. *Hum Reprod* 1999; **14**:2301–2312.
26. Aarabi M, Balakier H, Bashar S, Moskovtsev SI, Sutovsky P, Librach CL, Oko R. Sperm content of postacrosomal WW binding protein is related to fertilization outcomes in patients undergoing assisted reproductive technology. *Fertil Steril* 2014; **102**:440–447.
27. Laemmli UK. Cleavage of structural proteins during the assembly of the head of bacteriophage T4. *Nature* 1970; **227**: 680–685.
28. Oko RJ, Jando V, Wagner CL, Kistler WS, Hermo LS. Chromatin reorganization in rat spermatids during the disappearance of testis-specific histone, H1t, and the appearance of transition proteins TP1 and TP2. *Biol Reprod* 1996; **54**:1141–1157.
29. Ferrer M, Rodriguez H, Zara L, Yu Y, Xu W, Oko R. MMP2 and acrosin are major proteinases associated with the inner acrosomal membrane and may cooperate in sperm penetration of the zona pellucida during fertilization. *Cell Tissue Res* 2012; **349**:881–895.
30. Chen HI, Sudol M. The WW domain of Yes-associated protein binds a proline-rich ligand that differs from the consensus established for Src homology 3-binding modules. *Proc Natl Acad Sci USA* 1995; **92**:7819–7823.
31. Barth AD, Oko R. Normal bovine spermatogenesis and sperm maturation. *In: Abnormal Morphology of Bovine Spermatozoa*. Ames: Iowa State University Press; 1989: 1–285.
32. Oko R, Maravei D. Protein composition of the perinuclear theca of bull spermatozoa. *Biol Reprod* 1994; **50**:1000–1014.
33. Oko R, Maravei D. Distribution and possible role of perinuclear theca proteins during bovine spermiogenesis. *Microsc Res Tech* 1995; **32**:520–532.
34. Clermont Y, Oko R, Hermo L. Cell and molecular biology of the testis. In: Desjardins C, Ewing L (eds.), *Cell Biology of Mammalian Spermatogenesis*. New York: Oxford University Press; 1993: 332–376.
35. Kierszenbaum AL. Spermatid manchette: plugging proteins to zero into the sperm tail. *Mol Reprod Dev* 2001; **59**:347–349.
36. Meistrich ML, Trostle-Weige PK, Russell LD. Abnormal manchette development in spermatids ofazh/azh mutant mice. *Am J Anat* 1990; **188**:74–86.
37. Russell LD, Russell JA, MacGregor GR, Meistrich ML. Linkage of manchette microtubules to the nuclear envelope and observations of the role of the manchette in nuclear shaping during spermiogenesis in rodents. *Am J Anat* 1991; **192**:97–120.
38. Hall ES, Eveleth J, Jiang C, Redenbach DM, Boekelheide K. Distribution of the microtubule-dependent motors cytoplasmic dynein and kinesin in rat testis. *Biol Reprod* 1992; **46**:817–828.
39. Kierszenbaum AL. Intramanchette transport (IMT): managing the making of the spermatid head, centrosome, and tail. *Mol Reprod Dev* 2002; **63**: 1–4.
40. Miller MG, Mulholland DJ, Vogl AW. Rat testis motor proteins associated with spermatid translocation (dynein) and spermatid flagella (kinesin-II). *Biol Reprod* 1999; **60**:1047–1056.
41. Aul RB, Oko R. The major subacrosomal occupant of bull spermatozoa is a novel histone H2B variant associated with the forming acrosome during spermiogenesis. *Dev Biol* 2002; **242**:268–280.

42. Lalli M, Clermont Y. Structural changes of the head components of the rat spermatid during late spermiogenesis. *Am J Anat* 1981; **160**:419–434.
43. Oko R, Clermont Y. Isolation, structure and protein composition of the perforatorium of rat spermatozoa. *Biol Reprod* 1988; **39**:673–687.
44. Oko R, Clermont Y. Origin and distribution of perforatorial proteins during spermatogenesis of the rat: an immunocytochemical study. *Anat Rec* 1991; **230**:489–501.
45. Oko R, Morales CR. A novel testicular protein, with sequence similarities to a family of lipid binding proteins, is a major component of the rat sperm perinuclear theca. *Dev Biol* 1994; **166**: 235–245.
46. Rougier JS, Albesa M, Abriel H, Viard P. Neuronal precursor cell-expressed developmentally down-regulated 4-1 (NEDD4-1) controls the sorting of newly synthesized Ca(V)1.2 calcium channels. *J Biol Chem* 2011; **286**:8829–8838.